ELSEVIER

Biophysical Chemistry 60 (1996) 111–117

Biophysical Chemistry

Heme geometry in the 10 K photoproduct from sperm whale carbonmonoxymyoglobin

Antonio Cupane [a,*], Eugenio Vitrano [a], Pal Ormos [b], G. Ulrich Nienhaus [c]

[a] *Istituto di Fisica and INFM, University of Palermo, via Archirafi 36, I-90123 Palermo, Italy*
[b] *Institute of Biophysics, Hungarian Academy of Sciences, H-6701 Szeged, Hungary*
[c] *Department of Physics, University of Illinois at Urbana-Champaign, Urbana, Illinois 61801-3080, USA*

Received 27 October 1995; revised 3 January 1996; accepted 4 January 1996

Abstract

We have measured the Soret band of the photoproduct obtained by complete photolysis of sperm whale carbonmonoxymyoglobin at 10 K. The experimental spectrum has been modeled with an analytical expression that takes into account the homogeneous bandwidth, the coupling of the electronic transition with both high and low frequency vibrational modes, and the effects of static conformational heterogeneity. The comparison with deoxymyoglobin at low temperature reveals three main differences. In the photoproduct, the Soret band is shifted to red. The band is less asymmetric, and an enhanced coupling to the heme vibrational mode at 674 cm^{-1} is observed. These differences reflect incomplete relaxation of the active site after ligand dissociation. The smaller band asymmetry of the photoproduct can be explained by a smaller displacement of the iron atom from the mean porphyrin plane, in quantitative agreement with the X-ray structure analysis. The enhanced vibrational coupling is attributed to a subtle heme distortion from the planar geometry that is barely detectable in the X-ray structure.

Keywords: Photolysis; Photolyzed carbonmonoxymyoglobin; Low temperature absorption spectroscopy; Vibrational coupling; Iron out-of-plane displacement; Heme doming

1. Introduction

The kinetics of CO rebinding after flash photolysis of carbonmonoxymyoglobin (MbCO) have been extensively studied as a model for the structure-dynamics-function relationships in protein reactions, both at room [1] and cryogenic temperatures [2,3]. In recent years, research has focused on the interplay between protein motions and the ligand binding reaction. Of particular interest and importance for understanding the function of proteins in general is the relaxation from an intermediate structure (Mb*) towards the equilibrium structure of deoxymyoglobin (Mb) [3–7]. Structural and spectroscopic properties of the metastable photoproduct (Mb*CO) obtained after flash photolysis of MbCO are crucial for the development of quantitative models of the ligand rebinding process. Because of the fast relaxation,

* Corresponding author. Tel. (+39-91) 6171708, fax. (+39-91) 6162461, e-mail cupane@cuc.unipa.it.

PII S0301-4622(96)00011-7

Mb*CO can only be probed with transient spectrometers at higher temperatures (200–300 K). At low temperature (ca. 10 K), however, the properties of Mb*CO can be conveniently probed with slow spectrometers as relaxation is completely inactivated and recombination of CO with Mb after photodissociation is very slow. Various spectroscopic techniques have been employed to elucidate the properties of the low temperature photoproduct, including visible, near-infrared and infrared absorption [7–13], resonance Raman [14–16] and extended X-ray absorption fine structure [17,18] spectroscopies. Recently, the X-ray structure of Mb*CO at ca. 20 K has been determined [19–21], thus providing a structural framework for the interpretation of spectroscopic data.

The Soret absorption is routinely used to monitor the kinetics of CO rebinding [3], and its line shape in Mb*CO at liquid helium temperatures has been investigated [22]. However, a quantitative analysis relating the Soret line shape to the structural properties of the photoproduct is lacking. In this work, we have measured the Soret band of the photoproduct obtained after complete photolysis of MbCO at 10 K and analyzed it within the theory of electron-vibration coupling recently applied to the Soret spectra of heme proteins [23]. In this theory, the effects of conformational heterogeneity are also taken into account [22–24].

We show that the subtle but clear differences between the spectra of Mb*CO and Mb at low temperature can provide quantitative information on the heme geometry in Mb*CO.

2. Materials and methods

2.1. Experimental

Lyophilized sperm whale metMb (Sigma Chemical, Co., St. Louis, MO) was dissolved in distilled deionized water. The protein solution was centrifuged and filtered through a 1.2 μm filter to give an approximately 8 mM stock solution. Further dilution in a 75% v/v glycerol–phosphate buffer solution (pH 7) yielded a final protein concentration of about 6 μM. The solution was loaded in a gas-tight metacrylate cuvette. Subsequently, the sample in the cuvette was saturated with CO and reduced with sodium dithionite solution, freshly prepared under anaerobic conditions. Immediately afterwards, the sample was placed in a liquid He storage cryostat (Model 8DT, Janis Research Co., Wilmington, MA) with quartz windows and cooled to 10 K. The temperature was regulated with a digital temperature controller (Model DRC 82 C, Lake Shore Cryotronics, Westerville, OH). The cryogenic setup was mounted on a Cary-14 spectrometer interfaced to an IBM PC/AT (On-line Instrument Systems, Inc., Jefferson, GA). Absorption spectra were measured between 350 and 500 nm with a resolution of 0.2 nm and a wavelength accuracy of 0.1 nm. They were digitized in intervals of 0.5 nm. Photolysis was achieved with white light from a 250 W tungsten lamp (Oriel Corp., Stamford, CT) passed through a 10 cm path length water filter to avoid sample heating.

2.2. Spectral analysis

A detailed description of the theoretical approach used to obtain an analytical expression for the Soret band profile has been given in Ref. [23]. Here, we report only a brief summary.

The absorption line shape is considered to arise from the convolution of three terms:

$$A(\nu) = L(\nu) \otimes G(\nu') \otimes P(\nu_0) \tag{1}$$

The first term, $L(\nu)$, is a sum of Lorentzians, which arises from the coupling of the (intrinsically Lorentzian) electronic transition with high frequency vibrational modes ($h\nu_i > k_B T$) of the matrix surrounding the chromophore. Making use of the so called 'standard assumptions' [25] this term can be expressed as:

$$L(\nu) = M\nu \sum_{\{m_i\}} \left[\prod_i^{N_h} \frac{S_i^{m_i} e^{-S_i}}{m_i!} \right] \times \frac{\Gamma}{\left[\nu - \nu' - \sum_i^{N_h} m_i \nu_i \right]^2 + \Gamma^2} \tag{2}$$

where M is a constant proportional to the square of the electric dipole moment, and Γ is a damping factor related to the finite lifetime of the electroni-

Table 1
Values of the parameters obtained by fitting the Soret band of Mb*CO and of Mb in terms of Eq. (1)

Protein	Γ (cm^{-1})	S_{200}	S_{370}	S_{674}	S_{1357}	$Q_0\sqrt{b}$ ($\mu^{-1/2}$)	$\delta\sqrt{b}$ ($\mu^{-1/2}$)	ν_{00} (cm^{-1})	σ (cm^{-1})
Mb*CO ($T = 10$ K)	180 ± 10	0.07 ± 0.02	0.31 ± 0.03	0.33 ± 0.01	0.08 ± 0.01	0.146 ± 0.006	$0.15 \pm .01$	22520 ± 7	86 ± 6
Mb ($T = 20$ K)	185 ± 7	0.04 ± 0.02	0.27 ± 0.02	0.24 ± 0.01	0.09 ± 0.01	0.178 ± 0.005	$0.15 \pm .01$	22626 ± 8	85 ± 4

cally excited state. The sum extends over all possible combinations of m_i phonon events in the various high frequency vibrational modes i. The linear coupling strength is represented by S_i. According to Eq. (2), the spectrum consists of a superposition of a series of Lorentzians that includes all possible combinations of multiphonon excitations of the various high frequency modes. The displacement of the individual Lorentzians from the zero phonon line position reflects the energy lost to the phonons.

The second term, $G(\nu')$, takes into account the coupling of the electronic transition with a 'bath' of low frequency modes of the system. Within the so called 'short times approximation' [26], it can be shown that such a coupling generates a Gaussian distribution of the fundamental frequency ν':

$$G(\nu') = \frac{1}{\sqrt{2\pi}\sigma} e^{-\frac{[\nu' - \nu_0]^2}{2\sigma^2}} \tag{3}$$

When the effects of coupling with both high and low frequency modes are taken into account, the spectral line shape is therefore given by a superposition of Voigtians (convolutions of Lorentzians and Gaussians).

The third term, $P(\nu_0)$, takes into account the inhomogeneous broadening of the Soret line that arises from conformational heterogeneity. The dominant source of disorder affecting the Soret transition is most likely associated with the linkage between the porphyrin, iron, and proximal histidine, and the most important structural coordinate is believed to be the displacement of the iron with respect to the mean heme plane [3,22]. Other relevant coordinates are the tilt angle θ and the azimuthal angle ϕ characterizing the geometry of the imidazole side chain of the proximal histidine with respect to the porphyrin [27]. We model the structural distribution with a single generalized coordinate Q, which mainly reflects the iron displacement from the heme plane [1]. We take this coordinate to be distributed according to a Gaussian:

$$P(Q) = \frac{\exp\left[\frac{-(Q - Q_0)^2}{2\delta^2}\right]}{\sqrt{2\pi}\delta} \tag{4}$$

where Q_0 is the mean position, and δ characterizes the width of the distribution.

A mapping between structural and spectral heterogeneity has been obtained [22–24] by assuming a quadratic dependence of the fundamental transition frequency (parameter ν_0 in Eq. (3)) upon the coordinate Q.

$$\nu_0(Q) = \nu_{00} + bQ^2 \tag{5}$$

The parameter b accounts for the dependence of the $\pi \rightarrow \pi^*$ transition energy upon the iron coordinates and reflects the electronic properties of the iron-porphyrin system (for a more detailed discussion see Refs. [22] and [23]). By inserting Eq. (5) into Eq. (4), one finally obtains:

$$P(\nu_0) = \frac{e^{-\frac{\left(\sqrt{\nu_0 - \nu_{00}} + Q_0\sqrt{b}\right)^2}{2\delta^2}} + e^{-\frac{\left(\sqrt{\nu_0 - \nu_{00}} - Q_0\sqrt{b}\right)^2}{2\delta^2}}}{2\delta\sqrt{2\pi b[\nu_0 - \nu_{00}]}} \tag{6}$$

[1] A somewhat different approach has been used recently to account for the effect of conformational heterogeneity on the line shape of the ν_{Fe-His} Raman band and on the near-infrared absorption band III in horse heart deoxymyoglobin [28,29]. In fact, these bands have been deconvoluted in terms of a discrete number of subbands attributed to different conformational substates of the Fe–His linkage. This approach does not seem adequate in the present case, also in view of the rather large homogeneous width of the Soret band (Γ ca. 180 cm^{-1}; see Table 1).

From Eq. (6), it can be seen that for unliganded myoglobin a Gaussian distribution of iron atom out of plane positions produces an asymmetric non-Gaussian distribution of electronic transition energies. This effect is mainly due to the position of the iron atom out of the mean porphyrin plane; it is responsible for the characteristic marked asymmetry of the Soret band of deoxy heme proteins.

Fitting parameters are M, Γ, S_i, σ, ν_0, $Q_0\sqrt{b}$ and $\delta\sqrt{b}$. The ν_i values of the high frequency modes are taken from resonance Raman (RR) spectra [30,31]; we consider the coupling with only four modes, namely: $\nu = 200$, 370, 674 and 1357 cm^{-1}. The 'mode' at 200 cm^{-1} is an effective mode accounting for the two lines observed in RR spectra at about 150 and 220 cm^{-1}; we recall that a limit to our resolution of vibronic structure is posed by the intrinsic (homogeneous) width of the Soret band that, as shown by the values of parameter Γ reported in Table 1, is about 180 cm^{-1}. An analogous 'average mode' approximation has been used successfully in Ref. [32] in the analysis of Raman excitation profiles (REPs) of cytochrome c; on the other hand, it can be shown that this approximation does not introduce artificial vibronic progressions in the optical line shape as long as $n\Delta\nu/2 \ll \Gamma$, where $\Delta\nu$ is the frequency difference between the modes and n is the order of the progression. In the present case, given the values of coupling constants reported in Table 1 and neglecting vibronic contributions smaller than 0.5%, only vibronic progressions up to $n = 2$ need to be considered, so that the above condition is amply fulfilled. The 'mode' at 370 cm^{-1} is also an average mode accounting for a spectral region characterized by several quasi degenerate peaks. 674 and 1357 cm^{-1} correspond to the well known ν_7 and ν_4; however, in view of the above argument, contributions to S_{674} coming from the coupling with the nearby modes at about 750 and 780 cm^{-1} cannot be excluded. Equal ν_i values have been used for deoxymyoglobin and for the photoproduct; in fact it has been shown by RR spectroscopy [14,15] that for the modes considered any frequency differences are less than 5 cm^{-1}, i.e. undetectable with optical spectroscopy. A Gaussian curve centered at 26500 cm^{-1} is added, in order to take into account contributions from the higher frequency N band [33,34].

3. Results and discussion

The Soret band of the 10 K photoproduct is shown in Fig. 1, together with the fit using the theoretical expression presented in the preceding section. The residuals are shown on an expanded scale. Excellent agreement between experimental and calculated band profile is obtained.

Fit parameters are compiled in Table 1, together with data for equilibrium deoxymyoglobin at low temperature. The values of coupling constants to the high frequency modes deserve some comments.

(i) We find S_{200} values in the range 0.04–0.07, in agreement with the room temperature value obtained from REP measurements [31]. Within the fitting errors, no differences are observed between equilibrium deoxymyoglobin and the photoproduct. The sensitivity of our method is insufficient to detect eventual differences between the relative intensities of the 233 and 240 cm^{-1} lines reported for the low temperature MbCO photoproduct [15].

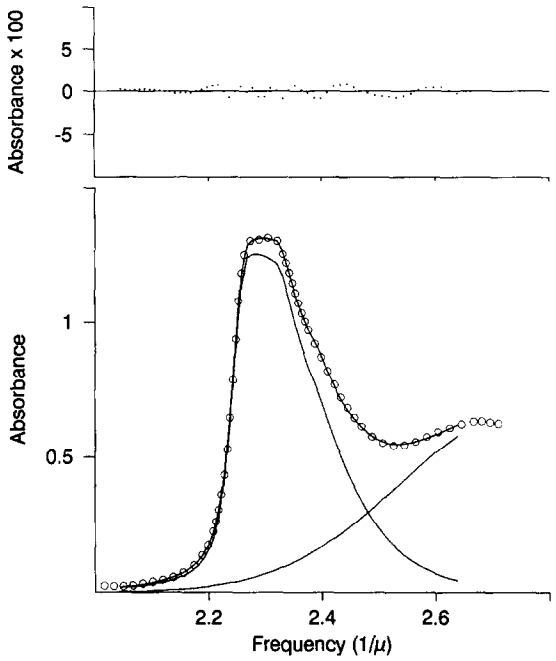

Fig. 1. Spectrum of Mb*CO at 10 K. Open circles represent the experimental points; the continuous lines represent the fit in terms of Eq. (1) and contributions from the N band. For the sake of clarity, not all experimental points have been reported. The residuals are given in the upper panel on an expanded scale.

(ii) For the average mode at 370 cm^{-1} we obtain coupling constants of 0.31 and 0.27 for the photoproduct and for static deoxymyoglobin, respectively. These values are in good agreement with the analogous room temperature ones of 0.21–0.24 obtained from REPs measurements for the average mode at 390 cm^{-1} of ferrocytochrome *c* [32]. The small increase observed for the photoproduct is within the limits of the fitting uncertainty.

(iii) For the mode at 674 cm^{-1}, we find *S* values of 0.33 (Mb*CO) and of 0.24 (Mb). The latter value is about 7 times larger than the analogous room temperature value (0.035) reported in Ref. [31]. We trace the origin of this discrepancy to the combination of the following effects: contributions from the nearby modes at 750 and 780 cm^{-1}, increase of coupling strength at low temperature, contributions to the low temperature Soret band arising from very weak underlying charge transfer transitions [22].

(iv) For the 1357 cm^{-1} mode, we obtain coupling constant values of 0.08–0.09, in excellent agreement with the room temperature value of 0.06.

Three main differences between the data sets relative to Mb*CO and to Mb are observed, the other parameters being unaffected. In Mb*CO:

1. the ν_{00} value is redshifted by about 140 cm^{-1} from ν_{00} of Mb;
2. the coupling with the vibrational mode at 674 cm^{-1} is enhanced;
3. parameter Q_0/b, related to the band asymmetry, is decreased by about 20%.

The three effects are better seen in Fig. 2a and Fig. 2b, where the Soret bands of the photoproduct and of low temperature equilibrium deoxymyoglobin are plotted after subtracting the contributions from the higher frequency *N* band. The redshift is clearly evident in Fig. 2a. To better inspect the other two effects we report the two spectra in Fig. 2b after redshifting the deoxy spectrum so as to overlap the red edges of bands. In Fig. 2b, enhanced coupling with the 674 cm^{-1} mode and lower band asymmetry in the photoproduct spectrum are clearly evident. We stress that the above effects cannot be attributed to incomplete photolysis (i.e. to a small fraction of MbCO still present in the photoproduct) since: (a) the Soret band of MbCO in 65% glycerol/water and at 10 K occurs at 23600 cm^{-1} [35] (arrow in Fig. 2b), i.e. at a frequency where the photoproduct spectrum does not show any shoulder and (b) the spectrum of the photoproduct was unchanged after several subsequent photolysing flashes.

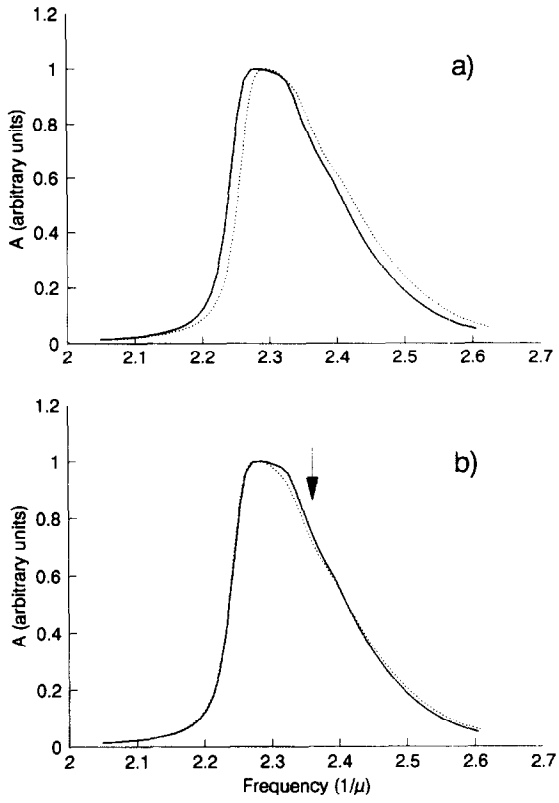

Fig. 2. (a) Soret band of Mb*CO (continuous line) and of Mb (dotted line) at 10 and 20 K, respectively. The profiles have been obtained from the experimental spectra by subtraction of the *N* band. (b) Same as in panel (a), after redshifting the profile relative to Mb by ca. 150 cm^{-1} so as to overlap the red edges of the bands. The arrow indicates the position of the Soret band of MbCO.

The redshift of the Mb*CO Soret band by about 140 cm^{-1} with respect to Mb has been reported previously [22,36]. The data in Table 1 show that this redshift is mainly due to a variation in parameter ν_{00} (i.e. in the zero phonon electronic transition frequency). Our line shape analysis reveals that the lower band asymmetry in the photoproduct (Fig. 2b) is caused by the lower value of the parameter Q_0/b (see Table 1), reflecting a smaller displacement of the iron atom out of the mean porphyrin plane, in agreement with the recently published X-ray structure of Mb*CO [19]. The agreement between optical and X-ray diffraction data is quantitative: both our

data in Table 1 and the X-ray data suggest a ca. 20% decrease of Fe-mean heme plane distance in Mb*CO with respect to Mb. The enhanced coupling with the mode at 674 cm^{-1} ($\nu_7 \equiv \delta C_\beta C_\alpha N + \nu C_\alpha C_\beta$, attributed to a totally symmetric A_{1g} vibration of the heme macrocycle that likely involves also the peripheral substituents) indicates that the heme geometry in the photoproduct is different from that of the fully relaxed deoxy derivative. From RR studies of metallooctaethylporphyrins, Kitagawa and coworkers [37] have suggested that the 674 cm^{-1} mode would give rise to an intense Raman line when the porphyrin ring is planar, while the intensity of this line would gradually diminish as the ring is domed. On this basis one could take the stronger coupling with the 674 cm^{-1} mode as an indication of a more planar heme structure in Mb*CO. X-ray crystallography is equivocal on this point. In fact, data from Ref. [19] suggest that, upon photolysis at 20 K, the movement of the pyrrole nitrogens out of the heme plane (i.e. heme doming) is complete; on the other hand, data from Ref. [20] suggest that at 40 K heme doming is not complete. The enhanced coupling of the Soret band with the ν_7 heme vibration has therefore to be attributed to a subtle variation of heme geometry that is barely detected by X-ray diffraction.

While conformational relaxation from the photoproduct structure Mb* to equilibrium Mb is thermally arrested at 10 K, it will become activated at higher temperatures. Srajer and Champion [22] observed a sharp transition in the Soret band position of the photoproduct Mb* to the equilibrium Mb position near 185 K. Detailed studies of the near-infrared band III at 760 nm in MbCO under continuous illumination [4] reveal a similar behavior. From the temperature dependence of the band area and position it was inferred that the protein is able to relax above about 160 K in glycerol/water mixtures. This temperature is near the glass transition temperature of the solvent, which indicates a strong coupling of protein and solvent motions. Indeed, it has been shown that protein motions are largely arrested in polymer or sugar matrices even at room temperature [2,38]. Frauenfelder and collaborators have coined the term 'slaved glass transition' to describe this dependence of the protein on the solvent dynamics [39].

In structural terms, the conformational relaxation in Mb*CO can be described as follows: after photodissociation of the CO, the iron shifts by a substantial fraction (ca. 80%) towards its equilibrium deoxy Mb position, and the heme geometry also changes. These motions are governed by electronic effects as well as by steric interactions between the proximal histidine and the heme [40] and do not involve major conformational changes. They therefore happen even at 10 K, and at room temperature very quickly (within a picosecond in HbCO) [41]. After this 'elastic' change, additional, slower relaxations occur, as reflected in the shift of band III in the near infrared over several decades in time [6]. Even though the subsequent shift of the iron has a much smaller amplitude, it may actually involve large changes in the rebinding barriers [7]. Molecular dynamics calculations by Karplus and collaborators [5] were also able to simulate an ultrafast relaxation similar to that of a heme–histidine–CO complex, plus an additional slower process that agrees with the time dependence of the shift of band III. The slower part of the protein relaxation involves large-scale rearrangements in the structure, including a tilt of the iron-histidine bond and a shift of the F helix towards the FG corner. These motions occur by displacement of solvent and are therefore arrested below the glass transition.

Band III is inhomogeneously broadened, and a mapping exists between the activation enthalpy for ligand rebinding and the wavenumber of a homogeneous component; this gives rise to the so called 'kinetic hole burning' effect [8]. A similar situation should also exist for the Soret band; moreover, one should expect to observe kinetic hole burning also for the other spectroscopic parameters that characterize the heme geometry (Q_0/b and S_{674}). However, an evaluation of the relative contributions of the heme geometry variations to the enthalpic barrier to ligand rebinding from the pocket remains unresolved by the present study and must await for accurate time-resolved studies of the Soret band line shape at various levels of ligand rebinding after photolysis.

Acknowledgements

The authors wish to thank Prof. L. Cordone and Dr. M. Leone for discussions and for reading the

manuscript. General indirect support from Comitato Regionale Ricerche Nucleari e Struttura della Materia (CRRNSM) to A.C. and E.V. is also acknowledged. This work was supported in part by a grant from the National Institutes of Health (GM 18051) to G.U.N.

References

[1] A. Ansari, C.M. Jones, E.R. Henry, J. Hofrichter and W.A. Eaton, Science, 256 (1992) 1796.
[2] R.H. Austin, K.W. Beeson, L. Eisenstein, H. Frauenfelder and I.C. Gunsalus, Biochemistry, 14 (1975) 5355.
[3] P.J. Steinbach, A. Ansari, J. Berendzen, D. Braunstein, K. Chu, B.R. Cowen, D. Ehrenstein, H. Frauenfelder, J.B. Johnson, D.C. Lamb, S. Luck, J.R. Mourant, G.U. Nienhaus, P. Ormos, R. Philipp, A. Xie and R.D. Young, Biochemistry, 30 (1991) 3988.
[4] G.U. Nienhaus, J.R. Mourant and H. Frauenfelder, Proc. Natl. Acad. Sci. USA, 89 (1992) 2902.
[5] K. Kuczera, J.C. Lambry, J.R. Martin and M. Karplus, Proc. Natl. Acad. Sci. USA, 90 (1993) 5805.
[6] T.A. Jackson, M. Lim and P.A. Anfinrud, Chem. Phys., 180 (1994) 131.
[7] G.U. Nienhaus, J.R. Mourant, K. Chu and H. Frauenfelder, Biochemistry, 33 (1994) 13413.
[8] B.F. Campbell, M.R. Chance and J.M. Friedman, Science, 238 (1987) 373.
[9] L. Cordone, A. Cupane, M. Leone and E. Vitrano, Biopolymers, 29 (1990) 639.
[10] F.G. Fiamingo and J.O. Alben, Biochemistry, 24 (1985) 7964.
[11] P. Ormos, D. Braunstein, H. Frauenfelder, M.K. Hong, S. Lin, T.B. Sauke and R.D. Young, Proc. Natl. Acad. Sci. USA, 85 (1988) 8492.
[12] P. Ormos, A. Ansari, D. Braunstein, B.R. Cowen, H. Frauenfelder, M.K. Hong, I.E.T. Iben, T.B. Sauke, P. Steinbach and R.D. Young, Biophys. J., 57 (1990) 191.
[13] J.R. Mourant, D.P. Braunstein, K. Chu, H. Frauenfelder, G.U. Nienhaus, P. Ormos and R.D. Young, Biophys. J., 65 (1993) 1496.
[14] D.L. Rousseau and P.V. Argade, Proc. Natl. Acad. Sci. USA, 83 (1986) 1310.
[15] M. Sassaroli, S. Dasgupta and D.L. Rousseau, J. Biol. Chem., 261 (1986) 13704.
[16] A.M. Ahmed, B.F. Campbell, D. Caruso, M.R. Chance, M.D. Chavez, S.H. Courtney, J.M. Friedman, I.E.T. Iben, M.R. Ondrias and M. Yang, Chem. Phys., 158 (1991) 329.
[17] T.Y. Teng, H.W. Huang and G.A. Olah, Biochemistry, 26 (1987) 8066.
[18] L. Powers, M. Chance, B. Campbell, J. Friedman, S. Khalid, C. Kumar, A. Naqui, K.S. Reddy and Y. Zhou, Biochemistry, 26 (1987) 4785.
[19] I. Schlichting, J. Berendzen, G.N. Phillips, Jr. and R.M. Sweet, Nature (London), 371 (1994) 808.
[20] T.Y. Teng, V. Srajer and K. Moffat, Nature Struct. Biol., 1 (1994) 701.
[21] H. Hartmann, S. Zinser, P. Komninos, R.T. Schneider, G.U. Nienhaus and F. Parak, Proc. Natl. Acad. Sci. USA, (1996) in press.
[22] V. Srajer and P.M. Champion, Biochemistry, 30 (1991) 7390.
[23] A. Cupane, M. Leone, E. Vitrano and L. Cordone, Eur. Biophys. J., 23 (1995) 385.
[24] V. Srajer, K.T. Schomacker and P.M. Champion, Phys. Rev. Lett., 57 (1986) 1267.
[25] P.M. Champion and A.C. Albrecht, Ann. Rev. Phys. Chem., 33 (1982) 353.
[26] C.K. Chan and J.B. Page, J. Chem. Phys., 79 (1983) 5234.
[27] J. Friedman, B.F. Campbell and R.W. Noble, Biophys. Chem., 37 (1990) 43.
[28] H. Gilch, W. Dreybrodt and R. Schweitzer-Stenner, Biophys. J., 69 (1995) 214.
[29] H. Gilch, R. Schweitzer-Stenner, W. Dreybrodt, M. Leone, A. Cupane and L. Cordone, Int. J. Quantum Chem., in press.
[30] T.G. Spiro, in A.B.P. Lever and H.B. Gray (Editors), Iron Porphyrins part II, Addison and Wesley, Reading, MA, 1983, p. 89.
[31] O. Bangcharoenpaurpong, K.T. Schomacker and P.M. Champion, J. Am. Chem. Soc., 106 (1984) 5688.
[32] K.T. Schomacker, O. Bangcharoenpaurpong and P.M. Champion, J. Chem. Phys., 80 (1984) 4701.
[33] A. Di Pace, A. Cupane, M. Leone, E. Vitrano and L. Cordone, Biophys. J., 63 (1992) 475.
[34] A. Cupane, M. Leone and E. Vitrano, Eur. Biophys. J., 21 (1993) 385.
[35] A. Cupane, M. Leone, E. Vitrano, L. Cordone, U.R. Hiltpold, K.H. Winterhalter, W. Yu and E.E. Di Iorio, Biophys. J., 65 (1993) 2461.
[36] K. Chu, P. Ormos, D. Ehrenstein, H. Frauenfelder, I. Kovacs, P.J. Steinbach and R.D. Young, Biophys. J., 59 (1991) 287a.
[37] T. Kitagawa, M. Abe, Y. Kyogoku, H. Ogoshi, E. Watanabe and Z. Yoshida, J. Phys. Chem., 80 (1976) 1181.
[38] S.J. Hagen, J. Hofrichter and W.A. Eaton, Science, 269 (1995) 959.
[39] A. Ansari, J. Berendzen, D. Braunstein, B.R. Cowen, H. Frauenfelder, M.K. Hong, I.E.T. Iben, J.B. Johnson, P. Ormos, T.B. Sauke, R. Scholl, A. Schulte, P.J. Steinbach, J. Vittitow and R.D. Young, Biophys. Chem., 26 (1987) 337.
[40] S.S. Stavrov, Biophys. J., 65 (1993) 1942.
[41] S. Franzen, J.C. Lambry, B. Bohn, C. Poyart and J.L. Martin, Nature Struct. Biol., 1 (1994) 230.